https://doi.org/10.15407/ujpe70.5.303

M.P. GORISHNYI

Department of Molecular Photoelectronics, Institute of Physics, Nat. Acad. of Sci. of Ukraine
(46, Nauky Ave., Kyiv 03028, Ukraine; e-mail: miron.gorishny@gmail.com)

DETERMINATION OF THE URBACH ENERGY E_u AND THE OPTICAL BAND GAP E_g IN SUBMICRON C_{60} AND C_{70} FULLERENE FILMS. DEPENDENCES OF E_u AND E_g OF THE FILMS ON THEIR THICKNESS IN THE RANGE 20—5000 nm

The long-wavelength spectral edge of the absorption coefficient α has been studied in detail within a spectral interval of 1.492–2.605 eV for C_{60} and C_{70} fullerene films with thicknesses ranging from 20 to 5000 nm. The values of the optical band gap E_g and the Urbach energy E_u in submicron C_{60} and C_{70} films are determined for the first time. It is found that the E_u-value decreases and the E_g-value increases, as the thickness of C_{60} films increases from 20 to 5000 nm, and the thickness of C_{70} films from 20 to 1000 nm. The highest, intermediate, and lowest E_g-values for C_{60} and C_{70} films are obtained using the Tauc, classical, and Cody methods, respectively. The average value of E_g, $\langle E_g \rangle$, coincides with the E_g-value obtained using the classical method. The average values of the parameter α_0, $\langle \alpha_0 \rangle$, within the exponential sections of the $\alpha(E)$ spectra are estimated; they turned out significantly larger for C_{70} films. The long-wavelength edge of the spectra $\alpha(E)$ is approximated by exponential dependences with the parameters $\langle \alpha_0 \rangle$, $\langle E_g \rangle$, and E_u.

Keywords: film, absorption spectrum, approximation, Gaussian function, C_{60} and C_{70} fullerenes, Urbach energy, optical band gap.

1. Introduction

Fullerenes C_{60} and C_{70} were discovered in 1985 [1]. A C_{60} molecule is a quasi-spherical cluster with I_h symmetry, which is formed by 12 pentagonal and 20 hexagonal faces with 60 carbon atoms at their vertices. In a C_{70} molecule with D_{5h} symmetry, two hemispheres of the C_{60} cluster are connected along the equatorial line by means of a belt consisting of 5 additional benzene rings; as a result, a C_{70} molecule has a quasi-ellipsoidal shape [2]. These materials are widely used as electron acceptors in organic solar cells [3]. In particular, C_{60} was used in solar cells [4], photovoltaic devices [5], photocatalysts [6], phototherapy [7], and biosensors [8]. C_{70} absorbs more strongly in the long-wave spectral interval of 1.771–2.480 nm, and it is suitable for replacing C_{60} in solar cells [9].

The photoelectric properties of bulk heterojunctions based on C_{60} and C_{70} derivatives with non-aromatic and tetracyclic aryl substituents (electron acceptors) incorporated into the PTB7-Th polymer matrix (an electron donor) were studied. The highest performance was observed for the indicated derivatives with monocyclic and bicyclic aromatic fragments. In particular, the open circuit voltage V_{oc} was equal to 0.8 V, and the short circuit current density J_{sc} to 10 mA/cm^2 [10].

According to mass spectrometry data [11], during the process of fullerene synthesis, molecules with different numbers of carbon atoms are formed. The main components of this mixture are the most stable molecules C_{60} and C_{70}. In work [12], the dynamics of changes in the composition of C_{60}/C_{70} films during their thermal deposition in vacuum was studied using the absorption spectra of C_{60}, C_{70}, and the C_{60}/C_{70} mixture.

Citation: Gorishnyi M.P. Determination of the Urbach energy E_u and the optical band gap E_g in submicron C_{60} and C_{70} fullerene films. Dependences of E_u and E_g of the films on their thickness in the range 20—5000 nm. *Ukr. J. Phys.* **70**, No. 5, 303 (2025). https://doi.org/ 10.15407/ujpe70.5.303.

Tauc *et al.* [13] described indirect electronic transitions between the extended energy states in the valence and conduction bands of amorphous germanium (a-Ge) films using the relationship $\omega^2\varepsilon_2 \sim (h\omega - E_g)^2$, where ω is the cyclic light frequency, ε_2 is the imaginary part of the complex dielectric function ε, $h\omega$ is the energy of light photon, and E_g is the optical band gap width. The value of E_g was determined by extrapolating the straight-line section in the dependence $h\omega(\varepsilon_2)^{1/2} = f(h\omega)$ to the zero ordinate value. Using the photothermal deflection and transmission spectroscopy methods, the distribution of localized states in the band gap of the films of amorphous silicon-based alloys (hydrogenated a-SiC and a-SiGe) 0.52–1.28 μm in thickness was studied. In the dependence $\log\alpha = f(hv)$, three regions in the absorption edge of those films were distinguished: the defect region (1.0–1.5 eV), the Urbach tail (1.5–1.9 eV), and the region of transitions between the extended states near the edges of the valence and conduction bands (1.9–2.2 eV). For the a-SiC and a-SiGe films, the values of E_g and the Urbach energy E_u were found to equal 1.79–2.17 eV and 58–115 meV, respectively [14].

The absorption edge of C_{60} films is similar to that of the films based on amorphous Si (a-SiC and a-Si : H). A vibronic structure (resonances at 1.51, 1.68, 1.83, 1.93, and 2.00 eV) was observed in the band gap of C_{60} films. For these films, $E_g = 1.64$ eV and $E_u = 61$ meV [15,16]. The absorption edge of 1-μm C_{70} films is similar to that of a-Si : H/SiN films 1.6 μm in thickness. For C_{70}, the values $E_g = 1.65$ eV and $E_u = 55$ meV were obtained, which are close to their counterparts for a-Si : H/SiN (1.66 eV and 69 meV, respectively). In the photon energy interval $E < 1.6$ eV, the C_{70} absorption shoulder at 1.5 eV is amazingly similar to the absorption of dangling silicon bonds in a-Si : H/SiN [17].

Under the external pressure action, an increase in the magnitude and a red shift of the absorption edge in polycrystalline granules of the C_{60}/C_{70} mixture were observed. The value of E_g decreases at that and approaches zero at a pressure of 20.5 GPa. After removing this pressure, the absorption edge in those granules is restored to its original form, which testifies to the absence of destruction of C_{60} and C_{70} molecules. It is assumed that, at pressures $\geq$21.5 GPa, C_{60}/C_{70} granules may have metallic conductivity [18]. For polycrystalline C_{70} granules, a red shift of the absorption edge without changing its slope was observed at pressures $\leq$10 GPa [19].

C_{60} films are characterized by three phases existing at different temperatures, T: orientational frozen phase 1 ($T \leq 150$ K), phase 2 with orientational disorder (150 K $< T \leq$ 260 K), and phase 3 with free rotation of C_{60} molecules (260 K $< T <$ 470 K). The values of E_g and E_u in C_{60} films 1.0–8.5 μm in thickness do not change in phase 1, change slowly in phase 2, and change quickly in phase 3. In the 8.5-μm C_{70} film, when the temperature grew, the value of E_g decreased and the value of E_u increased in phases 2 and 3. The corresponding values were 1.6–1.7 eV and 30–59 meV, respectively. The value of E_u is strongly affected by the orientational disorder of C_{60} molecules, whereas the O_2 intercalation does not change it. This fact means that the tail parameter E_u is an intrinsic characteristic of C_{60} films [20].

Preparation conditions strongly affect the structure, optical properties, and mechanical stresses in C_{60} films. Comprehensive optical and electron microscopic studies have shown that polycrystalline C_{60} films have a fundamental absorption edge at about 1.65 eV and the dependence of E_g on the mechanical stress magnitude P with $dE_g/dP = -2.8 \times \times 10^{-10}$ eV/Pa. In amorphous C_{60} films, mechanical stresses decrease, and the absorption edge is located at about 2.2 eV [21].

In works [13–21], the long-wave absorption edge was investigated, and the values of E_g and E_u in C_{60} and C_{70} films with thicknesses $d \geq 1$ μm were determined. However, there are no data on determining the values of E_g and E_u in C_{60} and C_{70} films with thicknesses $d < 1$ μm. For submicron C_{60} and C_{70} films, such studies are challenging and necessary for a deeper understanding of the operation of solar cells, sensors, and other devices based on various composites including thin C_{60} and C_{70} layers. The value of E_u governs the steepness of the long-wave absorption edge, and it is required to assess the degree of structuring in submicron C_{60} and C_{70} films induced by defect electronic states in the band gap. The value of E_g makes it possible to estimate the possible value of the absorption threshold for these films, which is very important for determining the efficiency of light energy conversion into electrical energy in solar cells and other similar devices based on composites with submicron C_{60} and C_{70} layers.

In this work, the values of E_g and E_u in submicron C_{60} and C_{70} films are determined for the first time in order to reveal possible features in the absorption edge behavior of those films. The absorption spectra of C_{60} and C_{70} films 20–5000 nm in thickness are analyzed in order to determine the dependence of the E_g- and E_u-values on the thickness of those films.

2. Direct and Indirect Electronic Transitions and Optical Band Gap in Semiconductors

According to the semiclassical theory, where the energy of electrons is quantized and photons are described as classical electromagnetic waves, the transition rate (the probability of transition per unit time) of an electron in a crystalline semiconductor from the valence to the conduction band is determined by the equation [22]

$$W = \frac{2\pi}{\hbar} |M|^2 N(E), \tag{1}$$

where M is the transition matrix element, $N(E)$ is the total electron-hole density of states, and $E = \hbar\omega = h\nu$ is the photon energy. In the case of direct (vertical) transition, the wave vector $\mathbf{k}$ of electron does not change. Then the absorption coefficient $\alpha(E < E_g) = 0$ and

$$\alpha(E \geq E_g) \sim (E - E_g)^{1/2}, \tag{2}$$

where E_g is the optical bandgap width of crystalline (polycrystalline) semiconductor. In this case, according to relationship (2), the value of E_g can be determined by extrapolating the straight-line section of the plot $\alpha^2 = f(E)$ to the point with the ordinate $\alpha^2 = 0$ and the abscissa $E = E_g$ [22, 23].

In the case of indirect (non-vertical) transition, the wave vector $\mathbf{k}$ of electron changes. Then, with regard for the law of conservation of momentum, the absorption of a photon by the electron is accompanied by the absorption or emission of a phonon. The rate of indirect transition W [Eq. (1)] is lower than that of direct transition. The corresponding absorption coefficient $\alpha = 0$ at the photon energy $E < E_g$, and

$$\alpha(E \geq E_g) \sim (E \pm \hbar\Omega - E_g)^2, \tag{3}$$

where the term $\hbar\Omega$ is the energy of the phonon at its emission ($+\hbar\Omega$) or absorption ($-\hbar\Omega$) [22, 24]. Since $\hbar\Omega \ll E$ and taking into account that $E = h\nu$, relationship (3) can be written in the form

$$\alpha^{1/2} = A(h\nu - E_g), \tag{4}$$

where A is a constant. Therefore, according to Eq. (4), the value of E_g for indirect transitions in crystalline (polycrystalline) semiconductors can be determined by extrapolating the straight-line section of the plot $\alpha^{1/2} = f(h\nu)$ to a point with the ordinate $\alpha^{1/2} = 0$ and the abscissa $h\nu = E_g$. Below, for convenience, the method of determining the value of E_g according to Eq. (4) will be called classical.

The absorption edge in amorphous germanium films is described by the Tauc relationship [13]

$$\omega^2\varepsilon_2 \sim (\hbar\omega - E_g)^2. \tag{5}$$

This relationship can be transformed into the equation

$$\omega^2\varepsilon_2 = A_1(\hbar\omega - E_g)^2, \tag{6}$$

where A_1 is a constant. The imaginary component of the dielectric function equals $\varepsilon_2 = 2nk$, where n and k are the refractive and absorption indices of the medium, respectively. The absorption coefficient of the medium equals $\alpha = 2\omega k/c$, where c is the speed of light in the medium [25]. After mathematical transformations, we obtain that $\varepsilon_2 = \alpha cn/\omega$. Substituting this expression for ε_2 into Eq. (6), taking into account that $\hbar\omega = h\nu$, and, after some mathematical transformations, we obtain:

$$(\alpha h\nu)^{1/2} = A_2(h\nu - E_g), \tag{7}$$

where $A_2 = A_1\hbar/(cn)$ is a constant. Equation (7) is used to describe the absorption edge of indirect electronic transitions in amorphous semiconductors.

Another approach to describe indirect transitions in amorphous semiconductors was proposed by Cody *et al.* [26] on the basis of their assumption that the transition dipole moment M [see Eq. (1)] is constant:

$$(\alpha/h\nu)^{1/2} = A_3(h\nu - E_g), \tag{8}$$

where A_3 is a constant. Based on the methods of Tauc and Cody, the value of E_g can be determined by extrapolating the straight-line sections of the plots of Eqs. (7) and (8) to the zero values of the ordinates $(\alpha h\nu)^{1/2}$ and $(\alpha/h\nu)^{1/2}$, respectively.

The spectral edge of the absorption coefficient α for amorphous semiconductors, in contrast to the sharp edge for their crystalline counterparts, is broad, and it can be conditionally divided into three regions: a) interband absorption with $\alpha > 10^4$ cm^{-1}, b) an exponential region (the Urbach tail) with $\alpha = (1 \div 10^3)$ cm^{-1}, and c) a weak absorption tail with $\alpha < 1$ cm^{-1}. The Urbach edge is a result of the electronic transitions among defect states located in the band gap near the upper edge of the valence band and the lower edge of the conduction band. The weak absorption tail may arise due to impurities. If we assume that defect states in an amorphous semiconductor are approximately described by parabolic bands, then the electron densities of states $N(E)$ near the edges of the valence and conduction bands can be extrapolated deeper into the forbidden gap. Then $E_g = E_{c\,\mathrm{opt}} - E_{v\,\mathrm{opt}}$, where $E_{c\,\mathrm{opt}}$ and $E_{v\,\mathrm{opt}}$ are the minimum and maximum of the extrapolated parabolic density bands near the conduction and valence band edges, respectively [27, 28].

The Urbach absorption tail is described by the following functional dependence [27]:

$$\alpha = \alpha_0 \exp\left(\frac{E - E_g}{E_u}\right), \tag{9}$$

where α_0 is a constant (measured in cm^{-1} units), and E_u is the Urbach energy. After taking the logarithm of Eq. (9), we obtain

$$\log \alpha = \log \alpha_0 + \frac{E - E_g}{E_u \ln 10},$$

where $\ln 10 \approx 2.3026$. Then, for two values, $\alpha(E_2)$ and $\alpha(E_1)$, the difference

$$\log\ \alpha(E_2) - \log \alpha(E_1) = \frac{E - E_g}{2.3026\, E_u},$$

and

$$E_u = \frac{E_2 - E_1}{2.3026\,[\log\ \alpha(E_2) - \log \alpha(E_1)]}. \tag{10}$$

So, the Urbach energy E_u is numerically equal to or inverse of the tangent of the slope angle of the straight section in the plot $\log \alpha = f(E)$ extrapolated to the ordinate or the abscissa axis, respectively.

In work [22], the $\alpha(E)$ spectra of Si, Ge, and GaAs crystals, powders, and amorphous specimens were studied in detail. The calculation of E_g for those semiconductors was carried out by analyzing the dependences of α (linear regression), α^2, $\alpha^{1/2}$, $(\alpha E)^{1/2}$, and $(\alpha/E)^{1/2}$ of the photon energy E, as well as using other methods. A new methodology for determining E_g via approximating the spectrum $\alpha(E)$ by the sigmoid-Boltzmann function was proposed.

In recent decades, the Tauc method became popular for studying direct and indirect transitions in crystalline and polycrystalline semiconductors. A necessary condition for using this method consists in that the absorption edge should be formed by only one interband transition between the parabolic bands. Quantum materials of various dimensions (two-dimensional, one-dimensional, and point-like) cannot be studied making use of the Tauc method, because they have strong band tails that overlap the fundamental absorption [27].

In this work, formulas (4), (7), (8) and (10) were used to determine the values of E_g and E_u in C_{60} and C_{70} films with various thicknesses.

3. Absorption Spectra of C_{60} and C_{70} Fullerene Films with Various Thicknesses

In works [9, 15–17, 20, 29], the original absorption spectra of C_{60} and C_{70} films with various thicknesses were presented in the coordinates D vs E, $\log D$ vs E, and $\log \alpha$ vs E, where D is the optical density, α is the absorption coefficient, and E is the photon energy. In this work, these spectra were transformed to the coordinates D vs E and reduced to the initial D_0-values within an interval from 0.001 to 0.005. Afterward, the reduced spectra $D(E)$ were recalculated into the coordinates α vs E. In our opinion, the spectra $\alpha(E)$ are more informative. For all those transformations, the computer program Origin was applied.

In work [12], the absorption spectra of C_{60} and C_{70} films 20 nm in thickness were approximated by Gaussian functions within the interval of 1.4–6.2 eV. For the C_{60} film, absorption bands at 1.999, 2.469 (the shoulder), and 2.774 eV were observed within the long-wavelength region of 1.4–3.0 eV. They were identified as the $h_u \to t_{1u}$ transition (the first band) and two $h_u \to t_{1g}$ transitions (the second and third bands). The absorption spectra of the C_{70} film in the interval of 1.4–3.0 eV revealed a broad band at 2.344 eV (the $e_2'' \to a_2''$ transition) and weak bands (shoulders) at 1.889 eV (the $e_1'' \to e_1''$or $a_2'' \to a_1''$ transition), 2.022 eV (a vibronic repetition of the

1.889-eV band with an intramolecular frequency of 1073 cm^{-1}), and 2.176 eV (the $a_2' \to e_1''$ transition).

At the photon energy $E = 1.999$ eV (the region of $h_u \to t_{1u}$ transition), the following values of the effective absorption coefficient α were obtained for C_{60} films with thicknesses of 20, 70, 900, ∼1000, and 5000 nm: 8.88×10^3, 6.33×10^3, 3.18×10^3, 0.85×10^3, and 6.60×10^3 cm^{-1}, respectively (see Fig. 1, curves *1* to *5*, respectively). A comparison of these spectra shows that the values of α decrease with the increasing thickness of the C_{60} films, i.e., the Bouguer–Lambert law is not fulfilled (curves *1* to *4*). For the 5000-nm C_{60} film (curve *5*), the value of α is larger than that for the C_{60} films with thicknesses of 900 and ∼1000 nm (curves *3* and *4*, respectively), and it is close to that for the C_{60} film with a thickness of 70 nm at $E = 1.999$ eV (curve *2*). The values of α for the C_{60} films with thicknesses of 20 and 70 nm are identical and equal to 3.17×10^3 cm^{-1} at $E = 1.796$ eV (curves *1* and *3*). An analysis of the absorption spectra $D(E)$ (they are not presented in this work) showed that the optical density D of C_{60} films with a thickness of ∼1000 nm is lower than that of 900-nm C_{60} films. These facts testify that the thickness of ∼1000 nm was overestimated for C_{60} films in works [15, 16]. Provided that the Bouguer–Lambert law is obeyed, it should be equal to 241 nm instead of the reported C_{60} film thickness of 900 nm.

At the photon energy $E = 1.999$ eV (the region of the $a_2'' \to a_1''$ transition), the following values of α were obtained for C_{70} films with thicknesses of 20, 160, ∼1000, and 1000 nm: 36.44×10^3, 19.32×10^3, 2.96×10^3, and 12.86×10^3 cm^{-1}, respectively (see Fig. 2, curves *1* to *4*, respectively). A decrease in the absorption coefficient α is observed, as the thickness of the C_{70} films increases from 20 to 1000 nm; i.e., the Bouguer–Lambert law is not obeyed, similarly to the C_{60} films. The thickness value of ∼1000 nm for the C_{70} film in works [15, 16] was overestimated. Our estimates showed that if the Bouguer–Lambert law is fulfilled, then, for the 1000-nm C_{70} film (curve *4*), it should be equal to 230 nm. For the C_{60} and C_{70} films with a thickness of 20 nm, the absorption coefficient α of the second film is 4.1 times larger, which testifies to a stronger absorption in the C_{70} films in the long-wavelength interval of 1.6–2.1 eV.

In work [15], bands at 1.51, 1.68, 1.83, 1.93, and 2.00 eV were observed at the long-wavelength edge of the absorption spectrum $\log \alpha = f(E)$ of the

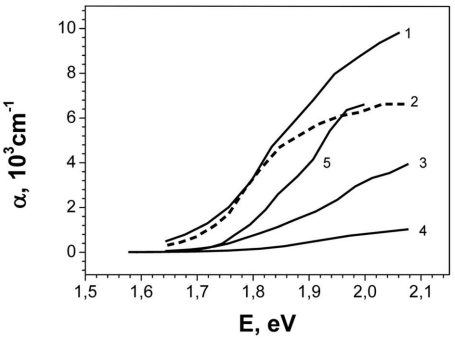

Fig. 1. Long-wavelength edges of the spectra of absorption coefficient α for C_{60} films with thicknesses of 20, 70, 900, ∼1000, and 5000 nm (curves *1* to *5*, respectively). The curves were plotted on the basis of original spectra taken from works [9] (curve *1*), [29] (curves *2* and *3*), [16] (curve *4*), and [20] (curve *5*)

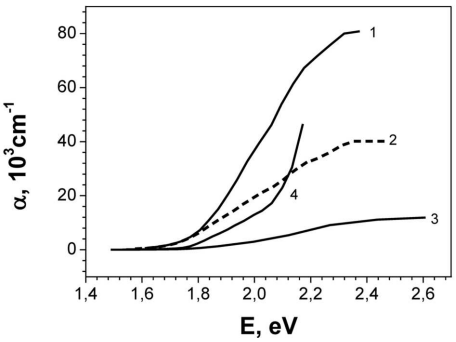

Fig. 2. Long-wavelength edges of the spectra of absorption coefficient α for C_{70} films with thicknesses of 20, 160, ∼1000, and 1000 nm (curves *1* to *4*, respectively). The curves were plotted on the basis of original spectra taken from works [9] (curve *1*), [17] (curves *2* and *4*), and [16] (curve *3*)

C_{60} film with a thickness of ∼1000 nm. It was assumed that these bands form a vibronic progression, with the $0 \to 0$ transition at 1.51 eV [15]. In order to confirm this assumption, we have studied here the long-wavelength edge of the absorption spectrum $\log \alpha = f(E)$ of the 5000 -nm C_{60} film, for which this structure should better manifest itself. The corresponding absorption spectrum, the baseline, and their difference are shown in Fig. 3, *a* (curves *1*, *2*, and *3*, respectively). Curve *3* was approximated using Gaussian functions, and the bands at 1.536, 1.640, 1.757, 1.855, and 1.939 eV are obtained (Fig. 3, *b*), which are close by their positions to the above bands, except for the band at 2.00 eV. The 2.00-eV band was observed in the absorption spectra of C_{60} films with smaller thicknesses and is close by its position to the

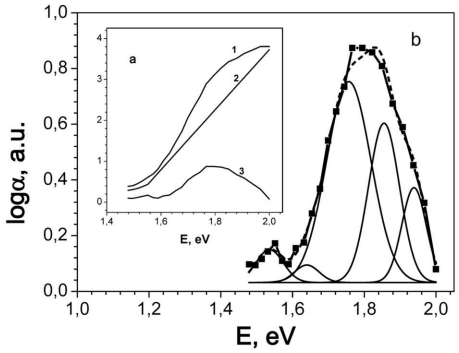

Fig. 3. Fitting of the long-wavelength edge of the spectrum of absorption coefficient α for the 5000-nm C_{60} film. Original spectrum, its baseline, and their difference are shown in the inset by curves *1* to *3*, respectively. All dependences are plotted in the semi-logarithmic scale. Initial data for curve *1* were taken from work [20]

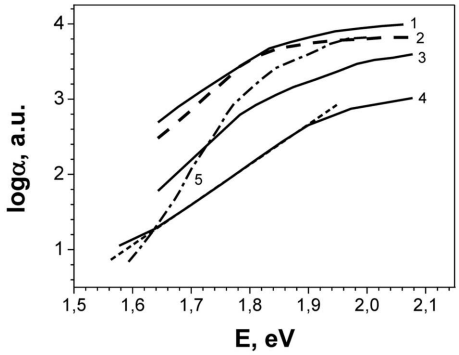

Fig. 4. Long-wavelength edges of the spectra of absorption coefficient α for C_{60} films with thicknesses of 20, 70, 900, ∼1000, and 5000 nm (curves *1* to *5*, respectively) in the semi-logarithmic scale. The short-dashed line demonstrates the straight-line fitting of the exponential section in curve *4*. Initial data for curve *1* were taken from work [9], for curves *2* and *3* from work [29], for curve *4* from work [16], and for curve *5* from work [20]

energy of 1.999 eV of the singlet $h_u \to t_{1u}$ transition [12]. The 1.536-eV band is close, by its position, to the energy of $0 \to 0$ triplet exciton C_{60}, which equals 1.50 eV [30]. Taking into account these data, it can be assumed that the long-wavelength absorption edge of C_{60} films is formed as a result of the superposition of the bands of triplet exciton vibronic progression at 1.536, 1.640, 1.757, 1.855, and 1.939 eV and the singlet exciton band at 1.999 eV.

The above-described reduction of the absorption coefficient α with the increasing thickness of the C_{60} and C_{70} films occurs due to the following reasons: a) the measurement accuracy of the film thickness in works [9, 15–17, 20, 29] was different, and b) the effective absorption decreases due to the increasing concentration of various molecular aggregates in the films with larger thicknesses. A detailed analysis of these reasons is not the aim of this work and may be the subject of a further research.

4. Determination of the Urbach Energy E_u From the Spectra of the Absorption Coefficient α for C_{60} and C_{70} Films with Vrious Thicknesses

The Urbach energy E_u is an important characteristic of C_{60} and C_{70} films. Its value can be used to determine the steepness of the long-wave absorption edge and assess the degree of structure ordering in these films.

To determine the value of E_u, Eq. (10) and the results of the straight-line approximation of the exponential sections in the $\alpha(E)$ spectra using the Origin program were applied. The absorption spectra $\log \alpha(E)$ of C_{60} films with thicknesses of 20, 70, 900, ∼1000, and 5000 nm are shown in Fig. 4 (curves *1* to *5*, respectively). On the semi-logarithmic scale, the exponential sections in those plots are observed as straight lines for all examined C_{60} films. For example, the short-dashed line corresponds to an extrapolated straight-line approximation of curve *4*. The $\log \alpha(E)$ plots for the C_{60} films with thicknesses of ∼1000 and 5000 nm (curves *4* and *5*, respectively) have S-like profiles. Three regions are observed in these plots: the beginning of weak absorption ($E <$ < 1.63 eV, $\log \alpha(E) \leq 1.26$ a.u.), exponential absorption (1.63 eV $< E <$ 1.89 eV, 1.26 a.u $< \log \alpha(E) \leq$ $\leq$ 2.62 a.u.), and absorption at the $h_u \to t_{1u}$ transition (1.89 eV $< E <$ 2.000 eV, 2.62 a.u. $< \log \alpha(E) \leq$ $\leq$ 3.81 a.u.).

The corresponding yield spectra were measured using the optical transmission and photothermal deflection spectroscopy methods [16, 20]. The latter method is more sensitive in the long-wavelength spectral interval and allows more accurate measurements to be carried out in the weak and exponential absorption spectral intervals of those films. The absorption spectra of the films 20, 70, and 900 nm in thickness (curves *1* to *3*, respectively) were measured only using the optical transmission spectroscopy method [9, 29]. For these films, the second and third absorption intervals were observed in this work.

Table 1. **Values of optical band gap E_g, Urbach energy E_u, and parameter $\langle\alpha_0\rangle$ for C_{60} and C_{70} fullerene films with various thicknesses**

Fullerene	d, nm	E_g, eV			$\langle E_g\rangle$, eV	E_u, MeV	$\log\alpha_1$, a.u.	$\log\alpha_2$, a.u.	E_1, eV	E_2, eV	$\langle\alpha_0\rangle$, cm^{-1}
		$(\alpha^* E)^{0,5}$	$(\alpha)^{0,5}$	$(\alpha/E)^{0,5}$							
C_{60}	20	1.596	1.586	1.576	1.586	82	2.700	3.502	1.645	1.796	244.71
	70	1.637	1.632	1.625	1.631	66	2.464	3.387	1.645	1.785	235.92
	900	1.653	1.649	1.645	1.649	60	1.722	2.923	1.645	1.811	56.32
	∼1000	1.665	1.658	1.651	1.658	81	1.276	2.439	1.638	1.856	24.00
	5000	1.675	1.675	1.672	1.674	35	1.215	2.889	1.632	1.767	54.40
C_{70}	20	1.663	1.652	1.640	1.652	79	2.805	4.037	1.614	1.837	1039.79
	160	1.604	1.595	1.582	1.594	77	2.442	3.758	1.562	1.795	420.14
	∼1000	1.662	1.637	1.608	1.636	79	1.002	2.811	1.492	1.808	67.77
	1000	1.683	1.678	1.673	1.678	57	2.410	3.526	1.673	1.820	279.31

The value of E_u was determined from the slope of the extrapolated approximation straight lines according to Eq. (10). The following values of E_u are obtained for the C_{60} films with thicknesses of 20, 70, 900, ∼1000, and 5000 nm: 82, 66, 60, 81, and 35 meV, respectively. A decrease in the value of E_u may indicate a decrease in the concentration of defect states in the band gap and, accordingly, an increase in the structure ordering degree in the C_{60} films, as their thickness increases from 20 to 5000 nm.

Figure 5 demonstrates the $\log\alpha(E)$ spectra of the C_{70} films with various thicknesses. The values of E_u for the C_{70} film ∼1000 nm in thickness were determined within the photon energy intervals $E =$ $= 1.492 \div 1.618$ and $(1.492 \div 1.808)$ eV (curve *3*); the obtained values were 61 and 79 meV, respectively. The former value coincides with that for the C_{60} film with a thickness of ∼1000 nm, which was obtained in works [15, 16]. In this work, the value of 79 meV, which was determined in a wider photon energy interval, was used for the analysis. Thus, the values of E_u are equal to 79, 77, 79, and 57 meV for the C_{70} films with thicknesses of 20, 160, ∼1000, and 1000 nm, respectively (curves *1* to *4*, respectively); i.e., E_u also decreases, as the thickness of C_{70}films increases from 20 to 1000 nm. Exceptions are the C_{60} and C_{70} films with a thickness of ∼1000 nm, for which $E_u = 81$ and 79 meV respectively. It can be assumed that thermally deposited C_{60} films with a lower degree of structural ordering were studied in works [15, 16].

The values of E_u and the coordinates of the beginning, $(E_1, \log\alpha_1)$, and end, $(E_2, \log\alpha_2)$, points of the coincidence of the extrapolated straight-line approximations with the plots $\log\alpha = f(E)$ for all examined C_{60} and C_{70} films are quoted in Table 1. It is found that the values of E_u determined using Eq. (10) and the straight-line approximation in the Origin program practically coincide for all films. For the straight-line approximation, the relative measurement error of E_u for the C_{60} and C_{70} films did not exceed 5%, with the correlation coefficient greater than 0.995. In this work, the values of E_u for all those films are obtained at D_0 within an interval from 0.001 to 0.005.

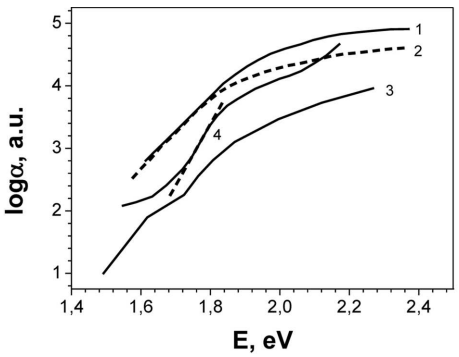

Fig. 5. Long-wavelength edges of the spectra of absorption coefficient α for C_{70} films with thicknesses of 20, 160, ∼1000, and 1000 nm (curves *1* to *4*, respectively) in the semi-logarithmic scale. The dashed line demonstrates the straight-line fitting of the exponential section in curve *4*. Initial data for curve *1* were taken from work [9], for curves *2* and *3* from work [17], and for curve *4* from work [16]

5. Determination of the Optical Bandgap width E_g in C_{60} and C_{70} Films

It was shown above that the value of the optical bandgap width E_g for indirect electronic transitions in amorphous and glassy semiconductors is determined using the Tauc and Cody methods by extrapolating the straight-line sections of the dependences of $(\alpha E)^{1/2}$ and $(\alpha/E)^{1/2}$, respectively, on the photon energy E to the zero ordinate values. The values of the corresponding abscissa values determine the value of E_g. To find the value of E_g for indirect electronic transitions in crystalline and polycrystalline semiconductors, the dependence $\alpha^{1/2} = f(E)$ is applied (earlier, we conditionally called this method classical).

The dependences of the quantities $(\alpha E)^{1/2}$, $\alpha^{1/2}$, and $(\alpha/E)^{1/2}$ on the photon energy E were plotted

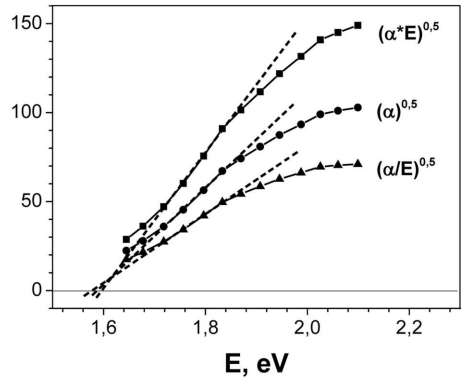

Fig. 6. Dependences of the quantities $(\alpha E)^{1/2}$, $\alpha^{1/2}$, and $(\alpha/E)^{1/2}$ on the incident photon energy E for the long-wavelength edge of the absorption spectrum for the 20-nm C_{60} film. The y-axis numerical scale is the same for all plots. The values of α and E_g are measured in cm^{-1} and eV units, respectively

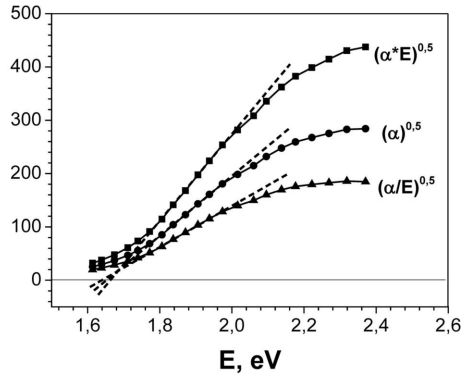

Fig. 7. The same as in Fig. 6, but for the 20-nm C_{70} film

on the basis of Eqs. (7), (4), and (8), respectively. For the C_{60} film with a thickness of 20 nm, these plots together with their extrapolated straight-line sections are shown in Fig. 6. The value of E_g was determined by extrapolating the straight-line section of the plot until it intersects the horizontal line with zero ordinate. The following values of E_g were obtained as the abscissas of those points: 1.596 eV for the function $(\alpha E)^{1/2}$ (the Tauc method), 1.586 eV for the function $\alpha^{1/2}$ (the classical method), and 1.576 eV for the function $(\alpha/E)^{1/2}$ (the Cody method). The largest value of E_g is given by the Tauc method, the intermediate one by the classical method, and the smallest one by the Cody method. The value $\langle E_g \rangle = 1.586$ eV is the average of the E_g values obtained in all three methods. It practically coincides with the E_g-value determined in the framework of the classical method. The relative deviations of the E_g-values from $\langle E_g \rangle$ are 0.63%, 0.00%, and −0.63%, respectively.

The plots of the quantities $(\alpha E)^{1/2}$, $\alpha^{1/2}$, and $(\alpha/E)^{1/2}$ on E for the 20-nm C_{70} film are shown in Fig. 7. The corresponding values obtained for E_g are 1.663, 1.652, and 1.640 eV. The relative deviations of the E_g-values from $\langle E_g \rangle = 1.625$ eV for the three methods are 0.67%, 0.00%, and −0.73%, respectively. A comparison demonstrates that the deviations of the E_g-values obtained in all three methods from $\langle E_g \rangle$ are close by magnitude for the C_{60} and C_{70} films.

The value of $\langle E_g \rangle$ for the C_{60} films increases from 1.586 to 1.674 eV as the film thickness increases from 20 to 5000 nm. For the C_{70} films, the $\langle E_g \rangle$-value increases from 1.594 to 1.678 eV, as their thickness increases from 160 to 1000 nm. An exception is the C_{70} film with a thickness of 20 nm, for which E_g is larger and is equal to 1.652 eV. If this value is considered as invalid, then it can be stated that the value of E_g also increases with the growth of the C_{70} film thickness from 20 to 1000 nm.

According to the results of the straight-line approximation in the Origin program, the relative measurement error of E_g in all C_{60} and C_{70} films did not exceed 5%, with the correlation coefficient being of at least 0.992. Therefore, the $\langle E_g \rangle$-values for the C_{60} and C_{70} films are close by magnitude and increase with the growth of film thickness within the intervals of 20–5000 and 20–1000 nm, respectively.

Electron microscopic studies of the structure of the 195-nm films of the C_{60}/C_{70} mixture showed

that it depends on the substrate type, being predominantly amorphous and filled with interspersed rounded and needle-shaped crystallites 50–200 nm in dimension [12]. Taking all that into account, it can be stated that, with the growth of the C_{60} and C_{70} film thickness, the intensity of crystallite formation, which is governed by the van der Waals interaction between the C_{60} and C_{70} molecules, increases in those layers of the indicated films that are remote from the substrate. As a result, the relative mass of the crystalline phase increases in the C_{60} and C_{70} films with larger thicknesses. The crystalline phase is characterized by a steeper slope of the long-wave absorption edge (a smaller value of E_u) and a larger value of E_g in comparison with the amorphous phase. Therefore, the growth of the structural ordering degree (the reduction of the E_u-value), which was described above, and the growth of the E_g-value as the thickness of the C_{60} and C_{70} films increases occur due to the enlargement of the crystalline phase contribution to light absorption in those films.

6. Determination of the Parameter $\langle\alpha_0\rangle$ for C_{60} and C_{70} films

After taking the logarithm of Eq. (9) and substituting E_g by $\langle E_g\rangle$, we obtain

$$\log\alpha_0 = \log\alpha - \frac{E - \langle E_g\rangle}{2.3026\,E_u}, \tag{11}$$

where the photon energy E belongs to the abscissa interval $[E_1, E_2]$ where the extrapolated straight-line approximations and the exponential sections of the dependences $\log\alpha = f(E)$ coincide. After exponentiating formula (11), we find the value of α_0. According to Eq. (11), the parameter $\log\langle\alpha_0\rangle = \log\alpha_0$ (i.e., $E = \langle E_g\rangle$) on the plot $\log\alpha = f(E)$ if $\langle E_g\rangle$ belongs to the interval $[E_1, E_2]$. This method can be conditionally called the direct potentiation. If $\langle E_g\rangle$ does not belong to the interval $[E_1, E_2]$, then it is necessary to calculate the value of α_0 using Eq. (11) where the photon energy E is taken from the interval $[E_1, E_2]$. By averaging those data, the average value $\langle\alpha_0\rangle$ of the quantity α_0 was determined.

An analysis of the data quoted in Table 1 showed that $\langle E_g\rangle$ belongs to the interval $[E_1, E_2]$ for the C_{60} films with thicknesses of ∼1000 and 5000 nm, and all C_{70} films. In this case, the $\langle\alpha_0\rangle$-value can be determined by means of the direct potentiation operation. For example, the direct potentiation brought us to the values $\alpha_0 = 23.83$ and 54.12 cm^{-1}, which are close by magnitude to the values $\langle\alpha_0\rangle = 24.00$ and 54.40 cm^{-1} (see Table 1) calculated using Eq. (11) for the C_{60} films with thicknesses of ∼1000 and 5000 nm, respectively. The relative difference $(\alpha_0 - \langle\alpha_0\rangle)/\langle\alpha_0\rangle$ for those films equals −0.7% and −0.5%, respectively.

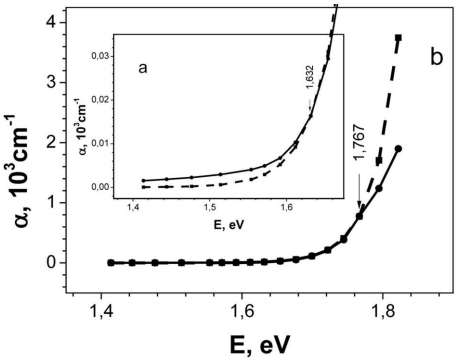

Fig. 8. The spectrum of absorption coefficient α for the 5000-nm C_{60} film (solid curves) and its approximation by exponential curves (dashed curves): in the interval of 1.414–1.822 eV and (inset) 1.414–1.654 eV. Initial data for the spectrum were taken from work [20]

As an example, in Fig. 8, the long-wavelength edge spectrum of the absorption coefficient α of the 5000-nm C_{60} film (the solid curve) is approximated by an exponential function (the dashed curve) calculated according to Eq. (11) with the following parameters: $\langle\alpha_0\rangle = 54.40$ cm^{-1}, $\langle E_g\rangle = 1.674$ eV, and $E_u = 0.035$ eV. One can see that the exponential curve and the spectrum $\alpha(E)$ coincide in the interval of photon energies $E = (1.632 \div 1.767)$ eV. Beyond this interval, the exponential curve passes below or above the spectrum α (the inset in Fig. 8 or Fig. 8 itself, respectively). The same is valid for the spectra $\alpha(E)$ of the C_{60} and C_{70} films with the thicknesses $d \geq 1$ μm if those spectra are approximated by exponential curves with the parameters $\langle\alpha_0\rangle$, $\langle E_g\rangle$, and E_u that are characteristic of these films (see Table 1). It was found that for the submicron C_{60} and C_{70} films, the approximated exponential curves coincide with the corresponding spectra $\alpha(E)$ in the intervals $E_1 \leq E \leq E_2$ and pass above them if $E > E_2$.

The interval of weak absorption (1.4–1.6 eV) in the oroginal spectra of submicron C_{60} and C_{70} films was shown in works [17, 29] as a horizontal straight line. This interval corresponds to the condition $E < E_1$. We may assume that for submicron C_{60} and C_{70} films, the approximated exponential curve for

this interval will pass below the spectrum $\alpha(E)$, as in the case of the 5000-nm C_{60} film (Fig. 8, the inset).

7. Comparison of the E_g- and E_u-Values Obtained in This Work for C_{60} and C_{70} Films with Various Thicknesses and the Corresponding Literature Data

The focus of scientific interest is to analyze the dependence of the E_g- and E_u-values on the thickness of C_{60} and C_{70} films. Three methods for determining the value of E_g have been proposed under the common name "Tauc equation". They are distinguished by the quantity–$(\alpha E)^{1/2}$, $\alpha^{1/2}$, or $(\alpha/E)^{1/2}$–whose dependence on the incident photon energy $E = hv$ is considered [17]. In this work, these methods correspond to Eqs. (7), (4), and (8), and, according to the data of work [22], are classified as the Tauc, classical, or Cody methods, respectively.

In this work, the values of E_g and E_u for C_{60} films with thicknesses of 20, 70, and 900 nm and C_{70} films with thicknesses of 20 and 160 nm were determined for the first time. For the examined C_{60} films, the average value $\langle E_g \rangle$ was found to equal 1.586, 1.631, and 1.649 eV, respectively, and the parameter E_u to 82, 66, and 60 meV, respectively. The $\langle E_g \rangle$-values for the C_{70} films with submicron thickness are 1.652 and 1.594 eV, and the E_u-value are 79 and 77 meV, respectively (see Table 1).

The literature data and the results obtained of this work for C_{60} and C_{70} films are compared in Table 2. The results obtained of this work are shown in bold italics. In works [15, 16], the values of E_g and E_u for the C_{60} film with a thickness of ∼1000 nm were equal to 1.640 eV and 61 meV, respectively. These values are 1.1% and 24.7%, respectively, smaller than the corresponding values obtained in this work: 1.658 eV (the average value) and 81 meV, respectively. For the 5000-nm C_{60} film, the values of E_g and E_u reported in work [20] are 1.650 eV and 37 meV, respectively. These values differ by −1.4% and 5.7% from the values obtained in this work, namely, 1.674 eV (the average value) and 35 meV, respectively.

Table 2. **Comparison of literature and experimental E_g and E_u data for C_{60} and C_{70} films with various thicknesses**

Fullerene	d, nm	E_g, eV	Difference, %	E_u, MeV	Difference, %
C_{60}	***∼1000***	***⟨1.658⟩***		**81**	
	∼1000 [15, 16]	1.640	–1.1	61	–24.7
	5000	***⟨1.674⟩***		***35***	
	5000 [20]	1.650	–1.4	37	5.7
C_{70}	***1000 (Tauc)***	***1.683***		***57***	
	1000 (Tauc) [17]	1.660	–1.7	55	–3.5
	1000 (classical)	***1.678***		***57***	
	1000 (classical) [17]	1.650	–1.7	55	–3.5
	1000 (Cody)	***1.673***		***57***	
	1000 (Cody) [17]	1.640	–2.0	55	–3.5
	∼1000	***⟨1.636⟩***		***79***	
	∼1000 [16]	∼1.500	–8.31	–	–

For the C_{70} film with a thickness of 1000 nm, the E_g-values were determined using the Tauc, classical, and Cody methods. The corresponding obtained values are 1.660, 1.650, and 1.640 eV [17], which are 1.7%, 1.7%, and 2.0% smaller than their counterparts obtained in this work 1.683, 1.678, and 1.673 eV, respectively. The value $E_u = 55$ meV obtained in work [17] is 3.5% smaller than the value $E_u = 57$ meV obtained in this work. For the C_{70} film with a thickness of ∼ 1000 nm, the estimated value of E_g was about 1.5 eV [16], which is 8.31% smaller than the value obtained in this work: $\langle E_g \rangle = 1.636$ eV. In work [16], the value of E_u for C_{70} films was not determined. In this work, $E_u = 79$ meV.

Thus, the values of E_g obtained in this work are in good agreement with the corresponding literature data. Their relative difference did not exceed 2.0%, if we omit the relative difference of 8.31% for the estimated value $E_g \approx 1.5$ eV for the C_{70} film with a thickness of ∼1000 nm.

The values of E_u are in satisfactory agreement for the C_{60} films with thicknesses of 5000 and 1000 nm (the relative difference is 5.7% and −3.5%, respectively). For the C_{60} film with a thickness of ∼1000 nm, the relative difference for E_u is significant and equals −24.7%.

8. Conclusions

The long-wavelength edge of the spectra of the absorption coefficient $\alpha(E)$ in the spectral interval $E = (1.492 \div 2.605)$ eV for the films of fullerenes C_{60} and C_{70} with thicknesses ranging within an interval of 20–5000 nm has been studied in detail.

The values E_g and E_u for the C_{60} films with thicknesses of 20, 70, and 900 nm and the C_{70} films with thicknesses of 20 and 160 nm are determined for the first time. For the indicated C_{60} films, the average

value of E_g is $\langle E_g \rangle$ = 1.586, 1.631, and 1.649 eV, respectively; and E_u = 82, 66, and 60 meV, respectively. The $\langle E_g \rangle$-values for the C_{70} films with submicron thicknesses are 1.652 and 1.594 eV, respectively; and the E_u-values are 79 and 77 meV, respectively.

Based on the results obtained in this work and the literature data, it is found that the value of E_u decreases and the value of E_g increases as the thicknesses of the C_{60} and C_{70} films grow from 20 to 5000 nm and from 20 to 1000 nm, respectively. This fact testifies to the growth of the structural ordering degree and the enhancement of the contribution made by the crystalline phase to the light absorption in those films.

For the C_{60} and C_{70} films, the largest, intermediate, and smallest values of the optical bandgap width E_g were obtained using the Taus, classical, and Cody methods, respectively. Their average value $\langle E_g \rangle$ coincides with the E_g-value obtained using the classical method.

The average values of the parameter α_0 are evaluated for the exponential sections in the long-wavelength edge of the spectra $\alpha(E)$, and they are found to be substantially larger for the C_{70} films. This is a result of the stronger absorption by C_{70} molecules than by C_{60} ones. The value of $\log \langle \alpha_0 \rangle$ is equal to the ordinate of a point with the abscissa $E = \langle E_g \rangle$ provided that the $\langle E_g \rangle$-value falls within the abscissa interval $[E_1, E_2]$ of the points where the straight-line approximations and the exponential parts of the spectra $\log \alpha(E)$ coincide.

The long-wavelength edge of the spectra $\alpha(E)$ were approximated by exponential curves with the parameters $\langle \alpha_0 \rangle$, $\langle E_g \rangle$, and E_u. It is found that for all C_{60} and C_{70} films, the approximating exponential curve coincides with the spectrum $\alpha(E)$ at the photon energies $E_1 \le E \le E_2$ and passes above it at $E > E_2$. For the C_{60} and C_{70} films with the thicknesses $d \ge 1$ μm, this exponential curve is located below the spectrum $\alpha(E)$ at $E < E_1$.

This work was supported from the budget of the NAS of Ukraine (project No. 1.4.B/209).

1. H.W. Kroto, J.R. Heath, S.C. O'Brien, R.F. Curl, R.E. Smalley. C_{60}: buckminsterfullerene. *Nature* **318** (6042), 162 (1985).
2. A. Graja, J.-P. Farges. Optical spectra of C_{60} and C_{70} complexes. Their Similarities and differences. *Adv. Mater. Opt. Electron.* **8**, 215 (1998).
3. L. Benatto, C.F.N. Marchiori, T. Talka, M. Aramini, N.A.D. Yamamoto, S. Huotari, L.S. Roman, M. Koehler. Comparing C_{60} and C_{70} as acceptor in organic solar cells: Influence of the electronic structure and aggregation size on the photovoltaic characteristics. *Thin Solid Films.* **697**, 137827 (2020).
4. Y. Yi, V. Coropceanu, J.-L. Brédas. Exciton-dissociation and charge-recombination processes in pentacene/C_{60} solar cells: Theoretical insight into the impact of interface geometry, *J. Am. Chem. Soc.* **131** (43), 15777 (2009).
5. P. Brown, P.V. Kamat. Quantum dot solar cells. Electrophoretic deposition of CdSe–C_{60} composite films and capture of photogenerated electrons with $n C_{60}$ cluster shell. *J. Am. Chem. Soc.* **130** (28), 8890 (2008).
6. H. Yi, D. Huang, L. Qin, G. Zeng, C. Lai, M. Cheng, S. Ye, B. Song, X. Ren, X. Guo. Selective prepared carbon nanomaterials for advanced photocatalytic application in environmental pollutant treatment and hydrogen production, *Appl. Catal. B* **239**, 408 (2018).
7. P. Mroz, G.P. Tegos, H. Gali, T. Wharton, T. Sarna, M.R. Hamblin. Photodynamic therapy with fullerenes. *Photoch. Photobid. Sci.* **6** (11), 1139 (2007).
8. S. Afreen, K. Muthoosamy, S. Manickam, U. Hashim. Functionalized fullerene (C60) as a potential nanomediator in the fabrication of highly sensitive biosensors. *Biosens. Bioelectron.* **63**, 354 (2015).
9. S. Pfuetzner, J. Meiss, A. Petrich, M. Riede, K. Leo. Improved bulk heterojunction organic solar cells employing C_{70} fullerenes. *Appl. Phys. Lett.* **94** (22), 223307 (2009).
10. W. Mech, P. Piotrowski, K. Zarebska, K.P. Korona, M. Kaminska, M. Skompska, A. Kaim. The impact of the presence of aromatic rings in the substituent on the performance of C_{60}/C_{70} fullerene – based acceptor materials in photovoltaic cells. *J. Electron. Mater.* **51**, 6995 (2022).
11. H. Ajie, M.M. Alvarez, S.J. Anz, R.D. Beck, F. Diederich, K. Fostiropoulos, D.R. Kraetschmer, M. Rubin, K.E. Schriver, D. Sensharma, R.L. Whetten. Characterization of the soluble all-carbon molecules C_{60} and C_{70}. *J. Phys. Chem.* **94**, 8630 (1990).
12. Gorishnyi M.P. Surface morphology of the films of the C_{60}/C_{70} fullerene mixture. Identification of C_{60} and C_{70} in the C_{60}/C_{70} films using absorption spectra. *Ukr. J. Phys.* **68** (5), 318 (2023).
13. J. Tauc, R. Grigorovici, A. Vancu. Optical properties and electronic structure of amorphous Germanium. *Phys. Stat. Sol.* **15**, 627 (1966).
14. A. Skumanich, A. Frova, N.M. Amer. Urbach tail and gap states in hydrogenated a-SiC and a-SiGe alloys. *Solid State Commun.* **54** (7), 597 (1985).
15. A. Scumanich. Optical absorption spectra of carbon 60 thin films from 0.4 to 6.2 eV. *Chem. Phys. Lett.* **182** (5), 486 (1991).
16. A. Scumanich. Optical spectra of fullerenes: C_{60} a new amorphous semiconductor? *Mat. Res. Soc. Symp. Proc.* **270**, 299 (1992).

17. W. Zhou, S. Xie, S. Qian, T. Zhou, R. Zhao, G. Wang, L. Qian, W. Li. Optical absorption spectra of C_{70} thin films. *J. Appl. Phys.* **80** (1), 489 (1996).
18. V.K. Dolganov, O.V. Zharikov, I.N. Kremenskaja, K.P. Meletov, Yu.A. Ossipyan. High pressure study of the absorption edge of crystalline C_{60}/C_{70} mixture. *Solid State Commun.* **83** (1), 63 (1992).
19. K.P. Meletov, V.K. Dolganov, Yu.A. Ossipyan. Absorption spectra of fullerite C_{70} at pressures up to 10 GPa. *Solid State Commun.* **87** (7), 639 (1993).
20. T. Gotoh, S. Nonomura, H. Watanabe, S. Nitta, D. Han. Temperature dependence of the optical-absorption edge in C_{60} thin films. *Phys. Rev. B* **58** (15), 10060 (1998).
21. E.Yu. Kolyadina, L.A. Matveeva, P.L. Neluba, E.F. Venger. Analysis of the fundamental absorption edge of the films obtained from the C_{60} fullerene molecular beam in vacuum and effect of internal mechanical stresses on it. *Semicond. Phys. Quant. Electron. Optoelectron.* **18** (3), 349 (2015).
22. A.R. Zanatta. Revisiting the optical bandgap of semiconductors and the proposal unified methodology to its determination. *Sci. Rep.* **9**, 11225 (2019).
23. M. Fox. *Optical Properties of Solids* (Oxford Univ. Press, 2008), chap. 1–3 [ISBN: 978-0-19-850613-3].
24. P.Y.Yu, M. Cardona. *Fundamentals of Semiconductors* (Springer, Berlin, 1996), chap. 6 [ISBN: 3-540-61461-3].
25. A.R. Forouhi, I. Bloomer. Optical properties of crystalline semiconductors and dielectrics. *Phys. Rev. B* **38** (3), 1865 (1988).
26. G.D. Cody, B.G. Brooks, B. Abeles. Optical absorption above the optical gap of amorphous silicon hydride. Solar Energy Mater. **8** (1–3), 231 (1982).
27. J. Klein, L. Kampermann, B. Mockenhaupt, M. Behrens, J. Strunk, G. Bacher. Limitations of the Tauc plot method. *Adv. Funct. Mater.* **33**, 2304523 (2023).
28. N. Sharma, K. Prabakar, S. Ilango, S. Dash, A.K. Tyagi. Optical band-gap and associated Urbach energy tails in defected AIN thin films grown by ion beam sputter deposition: Effect of assisted ion *energy. Adv. Mater. Proc.* **2** (5), 342 (2017).
29. W. Krätschmer, L. Lamb, K. Fostiropoulos, D.R. Huffman. Solid C_{60}: a new form of carbon. *Nature* **347**, 354 (1990).
30. S. Kazaoui, N. Minami, Y. Tanabe, M.J. Burne, A. Eilmes, P. Petelenz. Comprehensive analysis of intermolecular charge-transfer excited states in C_{60} and C_{70} films. *Phys. Rev. B* **58** (12), 7689 (1998).

Received 15.05.24
Translated from Ukrainian by O.I. Voitenko

М.П. Горішний

ВИЗНАЧЕННЯ ЕНЕРГІЇ УРБАХА E_u І ОПТИЧНОЇ ШИРИНИ ЗАБОРОНЕНОЇ ЗОНИ E_g СУБМІКРОННИХ ПЛІВОК ФУЛЕРЕНІВ C_{60} і C_{70}. ЗАЛЕЖНОСТІ E_u І E_g ЦИХ ПЛІВОК ВІД ЇХ ТОВЩИНИ В ДІАПАЗОНІ 20–5000 нм

Детально досліджено довгохвильовий край спектрів коефіцієнта поглинання α плівок фулеренів C_{60} і C_{70} товщиною 20–5000 нм в області 1,492–2,605 еВ. Вперше визначено величини ширини оптичної забороненої зони E_g і енергії Урбаха E_u субмікронних плівок C_{60} і C_{70}. Встановлено, що величина E_u зменшується, а величина E_g збільшується при зростанні товщини плівок C_{60} і C_{70} від 20 до 5000 нм і від 20 до 1000 нм відповідно. Найбільше, проміжне і найменше значення E_g плівок C_{60} і C_{70} одержано методами Таука, класичним і Коді відповідно. Середнє значення $\langle E_g \rangle$ співпадає з величиною E_g для класичного методу. Оцінено середні величини параметра $\langle \alpha_0 \rangle$ експоненціальних дільниць довгохвильових крайових спектрів $\alpha(E)$, які значно більші для плівок C_{70}. Довгохвильові крайові спектри $\alpha(E)$ апроксимовано експоненціальними лініями з параметрами $\langle \alpha_0 \rangle$, $\langle E_g \rangle$ і E_u.

Ключові слова: спектр поглинання, апроксимація, функція Гауса, фулерени C_{60} і C_{70}, енергія Урбаха, оптична ширина забороненої зони.